Unitarity bounds in the Higgs model including triplet fields with custodial symmetry

Mayumi Aoki[1]* and Shinya Kanemura[2]†

1: ICRR, University of Tokyo, Kashiwa 277-8582, Japan

2: Department of Physics, University of Toyama, 3190 Gofuku, Toyama 930-8555, Japan

Abstract

We study bounds on Higgs boson masses from perturbative unitarity in the Georgi-Machacek model, whose Higgs sector is composed of a scalar isospin doublet, a real and a complex isospin triplet fields. This model can be compatible with the electroweak precision data without fine tuning because of the imposed global $SU(2)_R$ symmetry in the Higgs potential, by which the electroweak rho parameter is unity at the tree level. All possible two-body elastic-scattering channels are taken into account to evaluate the S-wave amplitude matrix, and then the condition of perturbative unitarity is imposed on the eigenvalues to obtain constraint on the Higgs parameters. Masses of all scalar bosons turn out to be bounded from above, some of which receive more strict upper bounds as compared to that in the standard model (712 GeV). In particular, the upper bound of the lightest scalar boson, whatever it would be, is about 270 GeV.

PACS index : 12.60.Fr, 14.80.Cp

Keywords : Non-standard model, Partial-wave unitarity, Higgs boson mass bounds

*mayumi@icrr.u-tokyo.ac.jp

†kanemu@sci.u-toyama.ac.jp

1 Introduction

The nature of electroweak symmetry breaking remains unknown at the present status of our knowledge for high energy physics. In the standard model (SM), a scalar isospin doublet field, the Higgs field, is introduced to be responsible for spontaneous breakdown of electroweak gauge symmetry. Its vacuum expectation value (VEV) triggers the symmetry breaking, so that it provides origins of masses of weak bosons via the Higgs mechanism, and also does those of quarks and charged leptons via Yukawa interaction. Although the SM Higgs sector is simple, the Higgs sector could have a more complicated structure in the actual world. In particular, when the Higgs sector would play an additional role to explain phenomena which the SM cannot, it should necessarily be an extended form from the SM one. Therefore, experimental detection of the Higgs boson and precision measurements of its properties are extremely important not only to confirm our basic idea of electroweak symmetry breaking but also to determine details of the Higgs sector and further to outline the structure of new physics.

In constructing an extended Higgs sector, there are two important requirements from current experimental data. First of all, the data indicate that the electroweak rho parameter (ρ) is very close to unity. Second, flavor of quarks and charged leptons is (approximately) conserved in the neutral current. In the SM, these two conditions are satisfied respectively by the custodial symmetry which ensures $\rho = 1$ at the tree level, and by the Glashow-Iliopoulos-Maiani (GIM) mechanism which prohibits the tree-level flavor changing neutral current (FCNC). Needless to say that these experimental requirements must be respected in extended Higgs models which would appear in the low energy effective theory of a more fundamental theory beyond the SM.

Extension of the SM Higgs sector can be considered by including additional scalar isospin singlets, doublets and higher multiplets. It is known that additional singlets and doublets keep $\rho = 1$ at the tree level [1]. Radiative corrections can slightly deviate the rho parameter from unity, corresponding to explicit violation of the custodial symmetry in the dynamics in the loop. On the other hand, extension with higher multiplets such as triplets is usually problematic, predicting the rho parameter to be explicitly different from unity already at the tree level [2]. One way to avoid this problem is to make a fine-tuning on the size of vacuum expectation values of the triplet fields; i.e., to set tiny values on them. Another possibility is to impose the custodial symmetry to the Higgs sector, so that the rho parameter is predicted to be unity at the tree level. In 1985 Georgi and Machacek proposed such a model with one real triplet (Y=0) and one complex triplet (Y=2) in addition to the Higgs doublet [3]. Chanowitz and Golden have explicitly constructed the Higgs potential of this model [4]; i.e., imposing the custodial $SU(2)_{\rm V}$ symmetry to the potential, VEVs of all the isospin triplets become common, and then the tree-level value of the rho parameter is unity. They also have shown that the quantum correction from the scalar sector is stabilized by such a global symmetry, so that the rho parameter is corrected at the loop level only due to explicit $SU(2)_{\rm V}$ violation in the other sectors such as hypercharge interaction and Yukawa interaction, just like in the SM. Several phenomenological studies have been done on this model in Refs. [5, 6, 7, 8, 9, 10, 11, 12].

Generally in extended Higgs models, there are many free parameters in the Higgs potential, which spoil predictive power of the model. Hence, it is important to clarify allowed regions in the parameter space not only by using current experimental data but also by investigating theoretical consistencies such as perturbative unitarity [13, 14], vacuum stability and triviality [15]. This kind of study has been often developed to constrain parameters of the Higgs sector in the context of

the two-Higgs-doublet model [16, 17, 18, 19], and in a specific triplet model [20].

In this paper, we study bounds on Higgs boson masses from perturbative unitarity in the Georgi-Machacek (GM) model. The Higgs potential respects the global $SU(2)_R$ symmetry, so that the custodial $SU(2)_{\rm V}$ symmetry remains after the electroweak symmetry breaking ($SU(2)_L \otimes SU(2)_R \to SU(2)_{\rm V}$). There are ten physical scalar states, which can be expressed by a $SU(2)_{\rm V}$ 5-plet ($H_5^{++}, H_5^+, H_5^0, H_5^-, H_5^{--}$), a 3-plet ($H_3^+, H_3^0, H_3^-$) and two singlets $\tilde{H}_1^0$ and $\tilde{H}_1^{0\prime}$ [3]. The scalar components in the same multiplet are degenerate in mass at the tree level. In the Higgs potential of the GM model, explicit Z_2 violation can only appear in the trilinear scalar interaction, but they must be forbidden to avoid excessive magnitudes for masses of neutrinos. Neglecting such terms by imposing the Z_2 symmetry, all Higgs boson masses in this model are described in terms of the VEV, the mixing angles and the dimension-less coupling constants λ_i in the Higgs potential. This situation is somewhat similar to the two-Higgs-doublet model with the discrete Z_2 symmetry [21], in which perturbative unitarity gives upper bounds on all the Higgs boson masses [16].

In our analysis, all possible two-body elastic scattering channels (91-channels) are taken into account to evaluate the S-wave amplitude matrix in the GM model. Constraints on the Higgs parameters are obtained by imposing the condition of partial wave unitarity on the eigenmatrix of the S-wave amplitude. Masses of all scalar bosons turn out to be bounded from above, some of which receive much stronger bounds as compared to that in the SM (712 GeV). In particular, the mass of at least one of the charged Higgs bosons should be less than about 400 GeV. At least one of the neutral Higgs boson is lighter than 322 GeV. Furthermore, the upper bound of the lightest scalar boson, whatever it would be, can be about 269 GeV. We also find that by using the experimental constraints from $Zb\bar{b}$ results [11], the combined upper bound for the lightest Higgs boson is lower than 269 GeV, depending on what the lighest is. Therefore, the model can be well testable at current and future collider experiments.

In Sec. 2, a brief review of the GM model is given. The transition matrix for two-body elastic scatterings is calculated in the high-energy limit, and its eigenmatrix is obtained in Sec. 3. In Sec. 4, the condition of S-wave unitarity is imposed for the eigenmatrix of the transition matrix, and bounds on the Higgs boson masses are evaluated. Conclusions are presented in Sec. 5.

2 Georgi-Machacek Model

The GM model contains a complex $SU(2)_L$ doublet field ϕ (Y=1), a real $SU(2)_L$ triplet field ξ (Y=0) and a complex $SU(2)_L$ triplet field χ (Y=2) [3], and respects the global $SU(2)_R$ symmetry in the Higgs potential [4] . They can be described by the form of $SU(2)_L \otimes SU(2)_R$ multiplets Φ and Δ in the potential;

$$\Phi = \begin{pmatrix} \phi^{0*} & \phi^+ \\ \phi^- & \phi^0 \end{pmatrix}, \quad \Delta = \begin{pmatrix} \chi^{0*} & \xi^+ & \chi^{++} \\ \chi^- & \xi^0 & \chi^+ \\ \chi^{--} & \xi^- & \chi^0 \end{pmatrix}, \tag{2.1}$$

where $\phi = (\phi^+, \phi^0)^T$, $\xi = (\xi^+, \xi^0, \xi^-)^T$ and $\chi = (\chi^{++}, \chi^+, \chi^0)^T$, and $\phi^- = -(\phi^+)^*$, $\xi^- = -(\xi^+)^*$ and $\chi^- = -(\chi^+)^*$ [5]. The most general Higgs potential is given by

$$\begin{aligned} V &= m_1^2 {\rm Tr}(\Phi^\dagger\Phi) + m_2^2 {\rm Tr}(\Delta^\dagger\Delta) + \lambda_1 {\rm Tr}(\Phi^\dagger\Phi)^2 + \lambda_2 {\rm Tr}(\Delta^\dagger\Delta)^2 + \lambda_3 {\rm Tr}(\Phi^\dagger\Phi){\rm Tr}(\Delta^\dagger\Delta) \\ &\quad + \lambda_4 {\rm Tr}(\Delta^\dagger\Delta\Delta^\dagger\Delta) + \lambda_5 {\rm Tr}(\Phi^\dagger \frac{\tau_i}{2} \Phi \frac{\tau_j}{2}) {\rm Tr}(\Delta^\dagger T_i \Delta T_j) \end{aligned}$$

$$+\mu_1 \mathrm{Tr}(\Phi^\dagger \frac{\tau_i}{2} \Phi \frac{\tau_j}{2}) \Delta_P^{ij} + \mu_2 \mathrm{Tr}(\Delta^\dagger T_i \Delta T_j) \Delta_P^{ij} \ , \tag{2.2}$$

where τ_i are the 2×2 Pauli matrices and

$$\Delta_P = P^\dagger \Delta P, \qquad P = \begin{pmatrix} -1/\sqrt{2} & i/\sqrt{2} & 0 \\ 0 & 0 & 1 \\ 1/\sqrt{2} & i/\sqrt{2} & 0 \end{pmatrix} \ . \tag{2.3}$$

The neutral components of the doublet and the real and the complex triplets have the VEVs, v_ϕ, v_ξ, and v_χ, respectively, which are defined as

$$\phi^0 = \frac{v_\phi + \phi_r^0 + i\phi_i^0}{\sqrt{2}} \ , \tag{2.4}$$

$$\xi^0 = v_\xi + \xi_r^0 \ , \tag{2.5}$$

$$\chi^0 = v_\chi + \frac{\chi_r^0 + i\chi_i^0}{\sqrt{2}} \ . \tag{2.6}$$

After electroweak symmetry breaking, the custodial $SU(2)_{\rm V}$ symmetry remains in the Higgs sector ($SU(2)_L \times SU(2)_R \to SU(2)_{\rm V}$), by which the real and complex triplets have the same VEV, $v_\Delta \equiv v_\xi = v_\chi$. Consequently this leads to $\rho = 1$ at the tree level [4]. In this case the VEVs are constrained as $v^2 = v_\phi^2 + 8 v_\Delta^2$, where $v = (\sqrt{2} G_F)^{-\frac{1}{2}} \simeq 246$ GeV. Therefore, differently from usual triplet models, v_Δ can be of order 100 GeV in this model without explicit inconsistency with the experimental value of the rho parameter. It is convenient to introduce the doublet-triplet mixing angle θ_H,

$$\tan\theta_H = \frac{2\sqrt{2} v_\Delta}{v_\phi} \ . \tag{2.7}$$

The experimental constraint on θ_H is discussed in Ref. [11].

In the potential Eq.(2.2), the last two terms with the coupling constants μ_1 and μ_2 explicitly violate the discrete Z_2 symmetry under the transformation of $\Phi \to \Phi$ and $\Delta \to -\Delta$. Without the Z_2 symmetry, the model is allowed to have the mass terms for the neutrinos by assigning of lepton number -2 to the complex triplet field,

$$i (h_\nu)_{ab} \psi_{La}^T C \tau_2 \hat{\chi} \psi_{Lb} + \mathrm{h.c.}, \tag{2.8}$$

where $\hat{\chi} = \frac{\tau^i}{2} (P^\dagger \chi)^i$. In order to generate the tiny neutrino masses the Yukawa coupling h_ν should be fine-tuned to be very small as $h_\nu \sim \mathcal{O}(10^{-12})$ for the triplet VEV of order 100 GeV. Since we would like to avoid such fine tuning with respect to the neutrino masses, we require the discrete Z_2 symmetry in the Higgs potential and prohibit the last two terms in Eq.(2.2)[1]. Therefore, quarks and leptons couple to the $SU(2)_L$ doublet field Φ in the same way as the SM Yukawa coupling, but do not to the triplet Δ at the tree level. Because all the masses of quarks and leptons are obtained from the VEV in Φ, we do not have to worry about FCNC, and it is expected to appear at most at the same level as that in the SM. This property of the coupling to fermions would give an additional constraint on the value of the doublet-triplet mixing angle θ_H by $\tan\theta_H < \mathcal{O}(1)$, since large values of $\tan\theta_H$ ($\gg 1$) imply that the top-Yukawa coupling is much greater than $\mathcal{O}(1)$.

[1]The neutrino masses might be generated by any other mechanism (e.g. [22]). We shall discuss it elsewhere [23].

In the GM model, there are ten physical states in the Higgs sector, which are classified as a 5-plet $(H_5^{++}, H_5^+, H_5^0, H_5^-, H_5^{--})$, a 3-plet (H_3^+, H_3^0, H_3^-), and two singlets H_1^0 and $H_1^{0'}$ under the custodial $SU(2)_{\rm V}$ symmetry. These are given in terms of the original component fields and the doublet-triplet mixing angle θ_H as [5]

$$H_5^{++} = \chi^{++} \,, \tag{2.9}$$
$$H_5^{+} = (\chi^{+} - \xi^{+})/\sqrt{2} \,, \tag{2.10}$$
$$H_5^{0} = (2\xi_r^{0} - \sqrt{2}\chi_r^{0})/\sqrt{6} \,, \tag{2.11}$$
$$H_3^{+} = \cos\theta_H(\chi^{+} + \xi^{+})/\sqrt{2} - \sin\theta_H \phi^{+} \,, \tag{2.12}$$
$$H_3^{0} = i(-\cos\theta_H \chi_i^{0} + \sin\theta_H \phi_i^{0}) \,, \tag{2.13}$$
$$H_1^{0} = \phi_r^{0} \,, \tag{2.14}$$
$$H_1^{0'} = (\sqrt{2}\chi_r^{0} + \xi_r^{0})/\sqrt{3} \,. \tag{2.15}$$

The 5-plet components do not include the component fields from the isospin doublet field Φ, so that the states of the 5-plet do not couple to the fermions at the tree level. On the other hand, the 3-plet fields can couple to the fermions. Because of invariance under the custodial $SU(2)_{\rm V}$ symmetry, states in the different multiplet cannot mix each other.

All members in the same $SU(2)_{\rm V}$ multiplet are degenerate in mass at the tree level. The masses of the 5-plet and the 3-plet are respectively given by

$$m_{H_5}^2 = (\lambda_4 \sin^2\theta_H - \frac{3}{2}\lambda_5 \cos^2\theta_H) v^2 \,, \tag{2.16}$$
$$m_{H_3}^2 = -\frac{\lambda_5}{2} v^2 \,. \tag{2.17}$$

On the other hand, two $SU(2)_{\rm V}$ singlets can mix, and the mass matrix

$$\mathcal{M}^2_{H_1^0, H_1^{0'}} = \begin{pmatrix} 8\cos^2\theta_H \lambda_1 & \sqrt{\frac{3}{2}}\sin\theta_H \cos\theta_H (2\lambda_3 + \lambda_5) \\ \sqrt{\frac{3}{2}}\sin\theta_H \cos\theta_H (2\lambda_3 + \lambda_5) & \sin^2\theta_H (3\lambda_2 + \lambda_4) \end{pmatrix} v^2 \tag{2.18}$$

is diagonalized by introducing the mixing angle α. The eigenvalues correspond to the masses $m_{\tilde{H}_1^0}$ and $m_{\tilde{H}_1^{0'}}$ for the mass eigenstates $\tilde{H}_1^0$ and $\tilde{H}_1^{0'}$.

From Eqs.(2.16) - (2.18), the quartic couplings λ_i are expressed in terms of the masses and the mixing angles as

$$\lambda_1 = (m_{\tilde{H}_1^0}^2 \cos^2\alpha + m_{\tilde{H}_1^{0'}}^2 \sin^2\alpha)/(8v^2\cos^2\theta_H) \,, \tag{2.19}$$
$$\lambda_2 = (m_{\tilde{H}_1^0}^2 \sin^2\alpha + m_{\tilde{H}_1^{0'}}^2 \cos^2\alpha - m_{H_5}^2 + 3m_{H_3}^2\cos^2\theta_H)/(3v^2\sin^2\theta_H) \,, \tag{2.20}$$
$$\lambda_3 = (m_{\tilde{H}_1^{0'}}^2 - m_{\tilde{H}_1^0}^2)\cos\alpha\sin\alpha/(\sqrt{6}v^2\sin\theta_H\cos\theta_H) + m_{H_3}^2/v^2 \,, \tag{2.21}$$
$$\lambda_4 = (m_{H_5}^2 - 3m_{H_3}^2\cos^2\theta_H)/(v^2\sin^2\theta_H) \,, \tag{2.22}$$
$$\lambda_5 = -2m_{H_3}^2/v^2 \,. \tag{2.23}$$

The $SU(2)_{\rm V}$ 3-plet fields receive the constraints from the current data of $Z \to b\bar{b}$, $B_0 - \bar{B}_0$ and $K_0 - \bar{K}_0$ mixings [24, 25]. These data give bounds on the mass m_{H_3} with the mixing angle θ_H. The most stringent experimental constraint comes from $Z \to b\bar{b}$. The mass m_{H_3} is constrained to be smaller than 1 (0.5) TeV for $\tan\theta_H < 2$ (1).

Although the 5-plet fields do not couple to the fermions, the singly-charged state in the 5-plet has a characteristic coupling of $H_5^\pm W^\mp Z$, which only appears beyond the tree level in multi-Higgs-doublet models [26]. Experimental confirmation of a sizable coupling of $H_5^\pm W^\mp Z$ with $\rho \simeq 1$ should be a strong indication for the GM model[27]. This coupling is testable via the process $p\bar{p} \to W^\pm H^\mp$ at the Fermilab Tevatron [12], also via $pp \to W^{\pm *} Z^* X \to H^\pm X$ [28] and the decay process $H^\pm \to W^\mp Z$ [29] at the CERN LHC, and further via the processes $e^+e^- \to W^\mp H^\pm$ [8, 9, 30] and $e^+e^- \to \nu\bar{\nu} W^{\pm *} Z^* \to \nu\bar{\nu} H^\pm$ [31] at the ILC. Another striking feature of models with complex isospin-triplets, such as the GM model, the left-right symmetric model, the littlest Higgs model, and some models motivated by neutrino masses, is the appearance of doubly-charged states $H^{\pm\pm}$. At hadron colliders, such doubly-charged Higgs bosons are studied via the pair production mechanism [10, 32, 33] as well as the single production mechanism [33, 34] and the W-boson fusion mechanism [6, 35]. They can also be investigated at the ILC and its e^-e^-, $e^-\gamma$ and $\gamma\gamma$ option in various scenarios [36].

3 The S-matrix for two-body elastic scatterings

In this section, we calculate the transition matrix of elastic scatterings of two scalar-boson states in the GM model. The transition matrix $T(\varphi_1\varphi_2 \to \varphi_3\varphi_4)$ is equivalent to the S-wave amplitude $\langle\varphi_3\varphi_4|a^0|\varphi_1\varphi_2\rangle$ at high energies ($\sqrt{s} \gg m_W^2$), where φ_i represent longitudinally-polarized weak bosons or physical Higgs bosons of the model. The condition of partial wave unitarity is given for the S-wave amplitude matrix by [2, 13]

$$|\langle\varphi_3\varphi_4|a^0|\varphi_1\varphi_2\rangle| < \frac{1}{2}. \tag{3.24}$$

We employ this condition in the high energy limit to constrain the model parameters in the next section. Thanks to the equivalence theorem [37], the S-matrix elements in which longitudinally-polarized weak bosons are in initial and final states are equivalent to those in which these weak bosons are replaced by the corresponding Nambu-Goldstone bosons in the high energy limit [13]. In addition, in this limit, only quartic couplings (scalar contact interactions) of the Higgs-Goldstone couplings are relevant to the unitarity conditions, which can be translated into the bounds on the related Higgs-boson masses after Eq.(3.24) is imposed. Therefore, we here evaluate the matrix $\langle\varphi_3\varphi_4|a^0|\varphi_1\varphi_2\rangle$ taking into account all possible two-body scalar channels in the high energy limit, and obtain all the eigenstates and the eigenvalues.

Under $O(4)(\simeq SU(2)_L \otimes SU(2)_R)$, the field components of ϕ, χ and ξ are expressed by a $\underline{4}$ and a $\underline{9}$ representations as

$$\Psi_D = \left(\omega_1, \omega_2, \phi_r^0, \phi_i^0\right), \tag{3.25}$$

$$\Psi_T = \left(\chi_1, \chi_2, \chi_3, \chi_4, \xi_1, \xi_2, \chi_r^0, \chi_i^0, \xi_r^0\right), \tag{3.26}$$

where $\phi^+ = (\omega_1 + i\omega_2)/\sqrt{2}$, $\phi^0 = (\phi_r^0 + i\phi_i^0)/\sqrt{2}$, $\chi^{++} = (\chi_1 + i\chi_2)/\sqrt{2}$, $\chi^+ = (\chi_3 + i\chi_4)/\sqrt{2}$, $\chi^0 = (\chi_r^0 + i\chi_i^0)/\sqrt{2}$ and $\xi^+ = (\xi_1 + i\xi_2)/\sqrt{2}$. We consider all possible two-body scattering channels ($\Psi_a\Psi_b \to \Psi_c\Psi_d$) not only for the neutral two-body states as initial and final states but also for the singly-, the doubly-, the triply- and the quadruply-charged two-body states. There are totally 91 initial (or final) two-body states, in which 25 are the neutral, 36 are singly-charged, 22 are doubly-charged, 6 are triply-charged, and the last 2 are the quadruply-charged states. We construct the 91×91 transition matrix of high-energy S-wave amplitudes, and then calculate their eigenvalues.

The initial (final) two-body states can be treated separately as $\Psi_D\Psi_D$, $\Psi_T\Psi_T$ and $\Psi_D\Psi_T$. The high-energy S-wave amplitudes are block-diagonalized by the electric charge and also the discrete Z_2 symmetry ($\Phi \to \Phi$ and $\Delta \to -\Delta$). Each submatrix with respect to the $\Psi_D\Psi_D$ or $\Psi_T\Psi_T$ states can also be classified by irreducible decomposition of direct products of the representations for $O(4)$ as

$$\underline{4} \otimes \underline{4} = (1)_D \oplus (9) \oplus (6), \tag{3.27}$$

$$\underline{9} \otimes \underline{9} = (1)_T \oplus (44) \oplus (36). \tag{3.28}$$

The only singlet and symmetric representations,

$$(1)_a = \sum_{k=1} (\Psi_a^k)^2, \tag{3.29}$$

$$(s)^{ij} = \Psi_a^i \Psi_a^j - \frac{1}{N_a} \sum_{k=1} (\Psi_a^k)^2, \tag{3.30}$$

contribute to the scatterings of our interests, where $a = D$ or T; $i, j = 1{-}4$ and $s = 9$ for $a = D$,or $i, j = 1{-}9$ and $s = 44$ for $a = T$, and $N_D = 4$ and $N_T = 9$. For the $\Psi_D\Psi_T$ states which should be of the $\underline{4}\otimes\underline{9}$ representation, there is no singlet representation so that $O(4)$ cannot help for the classification. Furthermore, several additional discrete transformations can be used to further classify the states, which will be defined below.

Neutral channels

We outline further classification of the decomposed irreducible states for the case of the neutral 25 two-body channels (4 for $\Psi_D\Psi_D$, 11 for $\Psi_T\Psi_T$ and 10 for $\Psi_D\Psi_T$). For $\Psi_D\Psi_D$ states, we have the singlet state $(1)_D$ and the three neutral elements of $(9)^{ij}$ ($(9)^{33}$, $(9)^{44}$ and $(9)^{34}$), in which the C parity separates $(9)^{34}$ from the other states. After taking appropriate linear combination, we obtain two separate states under the transformation of $\phi_r \to \phi_i$ and $\phi_i \to -\phi_r$ as $((9)^{33} \pm (9)^{44})/\sqrt{2}$. Thus four eigenstates of the transition matrix for the neutral $\Psi_D\Psi_D \to \Psi_D\Psi_D$ channels are obtained [13].

Next, we consider $\Psi_T\Psi_T \to \Psi_T\Psi_T$ scatterings in which both the initial and final states are electrically neutral. In addition to the singlet state $(1)_T$, we have 10 neutral states from $(44)^{ij}$, in which $\{$ $(44)^{11}$+$(44)^{22}$, $(44)^{33}$+$(44)^{44}$, $(44)^{55}$+$(44)^{66}$, $(44)^{77}$, $(44)^{88}$ $\}$ are the diagonal element states ($i = j$), and $\{(44)^{35} + (44)^{46}$, $(44)^{36} - (44)^{45}$, $(44)^{78}$, $(44)^{79}$, $(44)^{89}\}$ are the off-diagonal element states ($i \neq j$). Among the diagonal element states, the linear combination $(44)^{77} - (44)^{88}$ has different property under the transformation of $\chi_r \to \chi_i$ and $\chi_i \to -\chi_r$. Then, linear combinations $\{$ $(44)^{11} + (44)^{22} + (44)^{77} + (44)^{88}$, $(44)^{33} + (44)^{44} + (44)^{55} + (44)^{66}$ $\}$ and $\{$ $(44)^{11} + (44)^{22} - (44)^{77} - (44)^{88}$, $(44)^{33} + (44)^{44} - (44)^{55} - (44)^{66}\}$ show different property under the transformation of $\chi^{++}\chi^{--} \leftrightarrow \chi^0\chi^0$, and $\chi^+\chi^- \leftrightarrow \xi^+\xi^-$. The first two states have completely the same property as that of the singlet state $(1)_T$, so that the appropriate linear combination of these three states give the three eigenstates. For the off-diagonal element states, we can separate them by using the C parity and the transformation of $\xi \to -\xi$, so that these states are block-diagonalized to two 2×2 submatrices and one singlet. By diagonalizing remained 2×2 matrices, we obtain all the eigenstates for the $\Psi_T\Psi_T \to \Psi_T\Psi_T$ channels.

In order to diagonalize all the $\Psi_D\Psi_D$ and $\Psi_T\Psi_T$ states, we take linear combinations of the eigenstates of $\Psi_D\Psi_D$ and $\Psi_T\Psi_T$ that have similar transformation properties. Consequently, all the

$\Psi_D\Psi_D$ and $\Psi_T\Psi_T$ states are completely separated, and the eigenvalues of the transition matrix for these channels are obtained.

Finally, classifying the ten $\Psi_D\Psi_T$ states by using the C transformation as well as some discrete transformations in a similar way to above, we completely diagonalized 25×25 scattering matrix for the electrically neutral two-body states.

The neutral states, $|A_i^0\rangle (i = 1 \sim 25)$, which give (at most 2×2) block-diagonal transition matrices are found as below:

$$
\begin{aligned}
|A_1^0\rangle &= (2\phi^+\phi^- + \phi_i^0\phi_i^0 + \phi_r^0\phi_r^0)/2\sqrt{2} \ , && (3.31)\\
|A_2^0\rangle &= (2\chi^{++}\chi^{--} + 2\chi^+\chi^- + 2\xi^+\xi^- + \chi_i^0\chi_i^0 + \chi_r^0\chi_r^0 + \xi_r^0\xi_r^0)/3\sqrt{2} \ , && (3.32)\\
|A_3^0\rangle &= (2\phi^+\phi^- - \phi_i^0\phi_i^0 - \phi_r^0\phi_r^0)/2\sqrt{2} \ , && (3.33)\\
|A_4^0\rangle &= (-2\chi^{++}\chi^{--} + \chi_i^0\chi_i^0 + \chi_r^0\chi_r^0)/2\sqrt{2} \ , && (3.34)\\
|A_5^0\rangle &= (\phi_i^0\phi_i^0 - \phi_r^0\phi_r^0)/2 \ , && (3.35)\\
|A_6^0\rangle &= (\chi^+\xi^- + \chi^-\xi^+ + \sqrt{2}\chi_r^0\xi_r^0)/2 \ , && (3.36)\\
|A_7^0\rangle &= \phi_r^0\phi_i^0 \ , && (3.37)\\
|A_8^0\rangle &= (\chi^+\xi^- - \chi^-\xi^+ - \sqrt{2}i\xi_r^0\chi_i^0)/(2i) \ , && (3.38)\\
|A_9^0\rangle &= (\chi_i^0\chi_i^0 - \chi_r^0\chi_r^0)/2 \ , && (3.39)\\
|A_{10}^0\rangle &= (2\chi^{++}\chi^{--} - \chi^+\chi^- - \xi^+\xi^- + \chi_i^0\chi_i^0 + \chi_r^0\chi_r^0 - 2\xi_r^0\xi_r^0)/3\sqrt{2} \ , && (3.40)\\
|A_{11}^0\rangle &= (2\chi^{++}\chi^{--} - 4\chi^+\chi^- - 4\xi^+\xi^- + \chi_r^0\chi_r^0 + \chi_i^0\chi_i^0 + 4\xi_r^0\xi_r^0)/6\sqrt{2} \ , && (3.41)\\
|A_{12}^0\rangle &= (\chi_r^0\chi_r^0 - \chi_r^0\chi_i^0)/\sqrt{2} \ , && (3.42)\\
|A_{13}^0\rangle &= (\chi^+\xi^- + \chi^-\xi^+ - \sqrt{2}\chi_r^0\xi_r^0)/2 \ , && (3.43)\\
|A_{14}^0\rangle &= (\chi^+\xi^- - \chi^-\xi^+ + \sqrt{2}i\xi_r^0\chi_i^0)/(2i) \ , && (3.44)\\
|A_{15}^0\rangle &= \chi_r^0\chi_i^0 \ , && (3.45)\\
|A_{16}^0\rangle &= \left\{2(\phi^+\chi^- + \phi^-\chi^+ + \phi^+\xi^- + \phi^-\xi^+) - \sqrt{2}(\phi_r^0\chi_r^0 + \phi_i^0\chi_i^0) - 2\phi_r^0\xi_r^0\right\}/3 \ , && (3.46)\\
|A_{17}^0\rangle &= (\phi_r^0\chi_r^0 - \phi_i^0\chi_i^0)/\sqrt{2} \ , && (3.47)\\
|A_{18}^0\rangle &= (\phi_i^0\chi_r^0 + \phi_r^0\chi_i^0)/\sqrt{2} \ , && (3.48)\\
|A_{19}^0\rangle &= \left\{2(\phi^+\chi^- - \phi^-\chi^+ - \phi^+\xi^- + \phi^-\xi^+) + \sqrt{2}i(\phi_i^0\chi_r^0 - \phi_r^0\chi_i^0) - 4i\phi_i^0\xi_r^0\right\}/(6i) \ , && (3.49)\\
|A_{20}^0\rangle &= \left\{\phi^+\chi^- + \phi^-\chi^+ + \phi^+\xi^- + \phi^-\xi^+ + \sqrt{2}(\phi_r^0\chi_r^0 + \phi_i^0\chi_i^0) + \phi_r^0\xi^0\right\}/3 \ , && (3.50)\\
|A_{21}^0\rangle &= \left\{\phi^+\chi^- - \phi^-\chi^+ - \phi^+\xi^- + \phi^-\xi^+ + \sqrt{2}i(\phi_r^0\chi_i^0 - \phi_i^0\chi_r^0) + i\phi_i^0\xi_r^0\right\}/(3i) \ , && (3.51)\\
|A_{22}^0\rangle &= \left\{\phi^+\chi^- - \phi^-\chi^+ - \phi^+\xi^- + \phi^-\xi^+ + 2\sqrt{2}i(\phi_i^0\chi_r^0 - \phi_r^0\chi_i^0) + 4i\phi_i^0\xi_r^0\right\}/(6i) \ , && (3.52)\\
|A_{23}^0\rangle &= \left\{\phi^+\chi^- + \phi^-\chi^+ + \phi^+\xi^- + \phi^-\xi^+ - 2\sqrt{2}(\phi_r^0\chi_r^0 + \phi_i^0\chi_i^0) + 4\phi_r^0\xi_r^0)\right\}/6 \ , && (3.53)\\
|A_{24}^0\rangle &= (\phi^+\chi^- + \phi^-\chi^+ - \phi^+\xi^- - \phi^-\xi^+)/2 \ , && (3.54)\\
|A_{25}^0\rangle &= (\phi^+\chi^- - \phi^-\chi^+ + \phi^+\xi^- - \phi^-\xi^+)/(2i) \ . && (3.55)
\end{aligned}
$$

The state $(1)_D$ and the three neutral linear-combined states from $(9)^{ij}$ respectively correspond to $|A_1^0\rangle$ and $\{|A_3^0\rangle, |A_5^0\rangle$ and $|A_7^0\rangle\}$. The state $(1)_T$ and the linear combined states from $(44)^{ij}$ correspond to $|A_2^0\rangle$ and $|A_i^0\rangle$ $(i = 4, 6, 8, 11 - 15)$, respectively. The first eight states block-diagonalize the transition matrix to four 2×2 submatrices, and the other seventeen states give eigenstates.

Singly-charged channels

There are eighteen singly-charged states with the electric charge +1 among all the two-body states. The charge conservation ensures that these states are composed of a subset among all the states with various electric charges. The corresponding high-energy transition matrix is consequently (block-) diagonalized by the following states:

$$
\begin{aligned}
|A_1^+\rangle &= (\phi^+\phi_r^0 + \phi^+\phi_i^0)/\sqrt{2}\ , && (3.56)\\
|A_2^+\rangle &= (\sqrt{2}\chi^{++}\chi^- + \chi^+\chi_r^0 + \chi^+\chi_i^0)/2\ , && (3.57)\\
|A_3^+\rangle &= (\phi^+\phi_r^0 - \phi^+\phi_i^0)/\sqrt{2}\ , && (3.58)\\
|A_4^+\rangle &= (\sqrt{2}\chi^{++}\xi^- + \xi^+\chi_r^0 - \xi^+\chi_i^0)/2\ , && (3.59)\\
|A_5^+\rangle &= (\sqrt{2}\chi^{++}\chi^- - \chi^+\chi_r^0 - \chi^+\chi_i^0 + 2\xi^+\xi_r^0)/2\sqrt{2}\ , && (3.60)\\
|A_6^+\rangle &= (\sqrt{2}\chi^{++}\xi^- - \xi^+\chi_r^0 + \xi^+\chi_i^0 + 2\chi^+\xi_r^0)/2\sqrt{2}\ , && (3.61)\\
|A_7^+\rangle &= (\sqrt{2}\chi^{++}\chi^- - \chi^+\chi_r^0 - \chi^+\chi_i^0 - 2\xi^+\xi_r^0)/2\sqrt{2}\ , && (3.62)\\
|A_8^+\rangle &= (\sqrt{2}\chi^{++}\xi^- - \xi^+\chi_r^0 + \xi^+\chi_i^0 - 2\chi^+\xi_r^0)/2\sqrt{2}\ , && (3.63)\\
|A_9^+\rangle &= (\xi^+\chi_r^0 + \xi^+\chi_i^0)/\sqrt{2}\ , && (3.64)\\
|A_{10}^+\rangle &= (\chi^+\chi_r^0 - \chi^+\chi_i^0)/\sqrt{2}\ , && (3.65)\\
|A_{11}^+\rangle &= (\chi^{++}\phi^- - 2\phi^+\xi_r^0 - \chi^+\phi_r^0 - \chi^+\phi_i^0 - \xi^+\phi_r^0 + \xi^+\phi_i^0)/3\ , && (3.66)\\
|A_{12}^+\rangle &= (\phi^+\chi_r^0 + \phi^+\chi_i^0 + \sqrt{2}\xi^+\phi_r^0 + \sqrt{2}\xi^+\phi_i^0)/\sqrt{6}\ , && (3.67)\\
|A_{13}^+\rangle &= (\phi^+\chi_r^0 - \phi^+\chi_i^0 + \sqrt{2}\chi^+\phi_r^0 - \sqrt{2}\chi^+\phi_i^0)/\sqrt{6}\ , && (3.68)\\
|A_{14}^+\rangle &= (4\chi^{++}\phi^- + 4\phi^+\chi_r^0 - \chi^+\phi_r^0 - \chi^+\phi_i^0 - \xi^+\phi_r^0 + \xi^+\phi_i^0)/6\ , && (3.69)\\
|A_{15}^+\rangle &= (\chi^+\phi_r^0 + \chi^+\phi_i^0 - \xi^+\phi_r^0 + \xi^+\phi_i^0)/2\ , && (3.70)\\
|A_{16}^+\rangle &= (\sqrt{2}\phi^+\chi_r^0 + \sqrt{2}\phi^+\chi_i^0 - \xi^+\phi_r^0 - \xi^+\phi_i^0)/\sqrt{6}\ , && (3.71)\\
|A_{17}^+\rangle &= (\sqrt{2}\phi^+\chi_r^0 - \sqrt{2}\phi^+\chi_i^0 - \chi^+\phi_r^0 + \chi^+\phi_i^0)/\sqrt{6}\ , && (3.72)\\
|A_{18}^+\rangle &= (2\chi^{++}\phi^- - \phi^+\xi_r^0 + \chi^+\phi_r^0 + \chi^+\phi_i^0 + \xi^+\phi_r^0 - \xi^+\phi_i^0)/3\ . && (3.73)
\end{aligned}
$$

The eighteen singly-charged states with the electric charge -1 can be obtained by the C transformation for the above states with the charge +1.

Doubly-charged channels

There are eleven doubly-charged two-body states with the electric charge +2. We can decompose the subset of the transition matrix for these states to at most 2×2 matrices by the following linear combination;

$$
\begin{aligned}
|A_1^{++}\rangle &= \phi^+\phi^+, && (3.74)\\
|A_2^{++}\rangle &= (\chi^+\xi^+ - \chi^{++}\xi_r^0)/\sqrt{2}\ , && (3.75)\\
|A_3^{++}\rangle &= \chi^+\chi^+, && (3.76)\\
|A_4^{++}\rangle &= (\chi^{++}\chi_r^0 - \chi^{++}\chi_i^0)/\sqrt{2}\ , && (3.77)\\
|A_5^{++}\rangle &= \xi^+\xi^+, && (3.78)\\
|A_6^{++}\rangle &= (\chi^{++}\chi_r^0 + \chi^{++}\chi_i^0)/\sqrt{2}\ , && (3.79)\\
|A_7^{++}\rangle &= (\chi^+\xi^+ + \chi^{++}\xi_r^0)/\sqrt{2}\ , && (3.80)
\end{aligned}
$$

$$
\begin{aligned}
|A_8^{++}\rangle &= (\phi^+\chi^+ + \phi^+\xi^+ + \chi^{++}\phi_r^0)/\sqrt{3}\,, && (3.81)\\
|A_9^{++}\rangle &= (\phi^+\chi^+ - \phi^+\xi^+ - \chi^{++}\phi_i^0)/\sqrt{3}\,, && (3.82)\\
|A_{10}^{++}\rangle &= (\phi^+\chi^+ + \phi^+\xi^+ - 2\chi^{++}\phi_r^0)/\sqrt{6}\,, && (3.83)\\
|A_{11}^{++}\rangle &= (\phi^+\chi^+ - \phi^+\xi^+ + 2\chi^{++}\phi_i^0)/\sqrt{6}\,. && (3.84)
\end{aligned}
$$

The corresponding doubly-charged two-body states with the charge -2 can be obtained by C transformation in the above states with the charge $+2$.

Triply-charged channels

There are three triply-charged states with the electric charge $+3$, and the subset of the transition matrix for the initial and final states can be diagonalized by the following eigenstates as

$$
\begin{aligned}
|A_1^{+++}\rangle &= \chi^{++}\phi^+, && (3.85)\\
|A_2^{+++}\rangle &= \chi^{++}\chi^+, && (3.86)\\
|A_3^{+++}\rangle &= \chi^{++}\xi^+. && (3.87)
\end{aligned}
$$

All the eigenstates with the opposite electric charge can be obtained by the C transformation of these eigenstates with the charge $+3$.

Quadruply-charged channels

Finally, we have only one quadruply-charged state for each electric charge of $+4$ and -4,

$$
\begin{aligned}
|A_1^{++++}\rangle &= \chi^{++}\chi^{++}, && (3.88)\\
|A_1^{----}\rangle &= \chi^{--}\chi^{--}. && (3.89)
\end{aligned}
$$

Eigenvalues of the transition matrix for all channels

In summary, the transition matrix T has been block-diagonalized as

$$
T = \begin{bmatrix}
T^0 & 0 & 0 & 0 & 0 & 0 & 0 & 0 & 0\\
0 & T^+ & 0 & 0 & 0 & 0 & 0 & 0 & 0\\
0 & 0 & T^- & 0 & 0 & 0 & 0 & 0 & 0\\
0 & 0 & 0 & T^{++} & 0 & 0 & 0 & 0 & 0\\
0 & 0 & 0 & 0 & T^{--} & 0 & 0 & 0 & 0\\
0 & 0 & 0 & 0 & 0 & T^{+++} & 0 & 0 & 0\\
0 & 0 & 0 & 0 & 0 & 0 & T^{---} & 0 & 0\\
0 & 0 & 0 & 0 & 0 & 0 & 0 & T^{++++} & 0\\
0 & 0 & 0 & 0 & 0 & 0 & 0 & 0 & T^{----}
\end{bmatrix}, \qquad (3.90)
$$

where block-diagonal transition submatrices for the neutral, the singly-charged, the doubly-charged, the triply-charged, and the quadruply-charged two-body states, T^0, $T^{\pm}$, $T^{\pm\pm}$, $T^{\pm\pm\pm}$, and $T^{\pm\pm\pm\pm}$, respectively, are given by

$$
T^0 = \mathrm{diag}(\mathbf{X_1}, \mathbf{X_2}, \mathbf{X_2}, \mathbf{X_2}, y_1, y_1, y_2, y_2, y_2, y_2, y_2, y_3, y_3, y_3, y_3, y_3, y_4, y_4, y_4, y_5, y_5)\,, \qquad (3.91)
$$

$$
\begin{aligned}
T^{\pm} &= \mathrm{diag}(\mathbf{X_3}, \mathbf{X_3}, y_6, y_6, y_7, y_7, y_2, y_2, y_3, y_3, y_3, y_4, y_4, y_4, y_4, y_5) \ , && (3.92)\\
T^{\pm\pm} &= \mathrm{diag}(\mathbf{X_4}, \mathbf{X_5}, \mathbf{X_5}, y_2, y_3, y_3, y_4, y_4) \ , && (3.93)\\
T^{\pm\pm\pm} &= \mathrm{diag}(y_3, y_2, y_2) \ , && (3.94)\\
T^{\pm\pm\pm\pm} &= 2y_2 \ . && (3.95)
\end{aligned}
$$

Here $\mathbf{X_i}$ are the 2×2 matrices whose eigenvalues $x_i^{\pm}$ are given by

$$
\begin{aligned}
x_1^{\pm} &= 12\lambda_1 + 22\lambda_2 + 14\lambda_4 \pm \sqrt{(12\lambda_1 - 22\lambda_2 - 14\lambda_4)^2 + 144\lambda_3^2} \ , && (3.96)\\
x_2^{\pm} &= 4\lambda_1 + 4\lambda_2 - 2\lambda_4 \pm \sqrt{(4\lambda_1 - 4\lambda_2 + 2\lambda_4)^2 + 4\lambda_5^2} \ , && (3.97)\\
x_3^{\pm} &= 4\lambda_2 + 4\lambda_1 \pm \sqrt{(4\lambda_2 - 4\lambda_1)^2 + 4\lambda_5^2} \ , && (3.98)\\
x_4^{\pm} &= 8\lambda_1 + 4\lambda_2 - 2\lambda_4 \pm \sqrt{(8\lambda_1 - 4\lambda_2 + 2\lambda_4)^2 + 8\lambda_5^2} \ , && (3.99)\\
x_5^{\pm} &= 12\lambda_2 + 14\lambda_4 \pm 2\sqrt{4\lambda_2^2 + 4\lambda_2\lambda_4 + 17\lambda_4^2} \ . && (3.100)
\end{aligned}
$$

The eigenvalues y_i are obtained as

$$
\begin{aligned}
y_1 &= 8\lambda_2 + 16\lambda_4 \ , && (3.101)\\
y_2 &= 8\lambda_2 + 4\lambda_4 \ , && (3.102)\\
y_3 &= 4\lambda_3 + \lambda_5 \ , && (3.103)\\
y_4 &= 4\lambda_3 - 2\lambda_5 \ , && (3.104)\\
y_5 &= 4(\lambda_3 + \lambda_5) \ , && (3.105)\\
y_6 &= 8\lambda_2 + 4(2 + \sqrt{2})\lambda_4 \ , && (3.106)\\
y_7 &= 8\lambda_2 + 4(2 - \sqrt{2})\lambda_4 \ . && (3.107)
\end{aligned}
$$

Although the transition matrix between initial and final two-body states is originally 91×91, the number of independent eigenvalues turns out to be only seventeen.

4 Unitarity bounds on the masses

In this section we analyze mass bounds on the Higgs bosons in the GM model, imposing the condition of perturbative unitarity in Eq. (3.24) to the transition matrix given in the previous section. Consequently we obtain seventeen inequations with respect to all the independent eigenvalues of the transition matrix T in Eq.(3.90) as

$$
|x_1^{\pm}|, |x_2^{\pm}|, |x_3^{\pm}|, |x_4^{\pm}|, |x_5^{\pm}|, |y_1|, |y_2|, |y_3|, |y_4|, |y_5|, |y_6|, |y_7| < 8\pi. \qquad (4.108)
$$

These eigenvalues are respectively given in Eqs. (3.96) - (3.107) as a combination of the dimensionless coupling constants λ_i ($i = 1 \sim 5$) in the Higgs potential, and λ_i are related to the Higgs boson masses through Eqs.(2.19)-(2.23), these constraints can be translated into the bounds on the masses $m_{\tilde{H}_1^0}$, $m_{\tilde{H}_1^{0\prime}}$, m_{H_3} and m_{H_5} and on the mixing angles θ_H and α.

We here show the numerical results on the Higgs mass bounds. Fig. 1 shows the allowed regions of the masses in the m_{H_3} - m_{H_5} plane (a), in the m_{H_3} - $m_{\tilde{H}_1^0}$ plane (b) and in the $m_{\tilde{H}_1^0}$ - $m_{\tilde{H}_1^{0\prime}}$ plane (c). We vary the Higgs boson masses in the range $m_{H_3}, m_{H_5}, m_{\tilde{H}_1^0}, m_{\tilde{H}_1^{0\prime}} < 1$ TeV

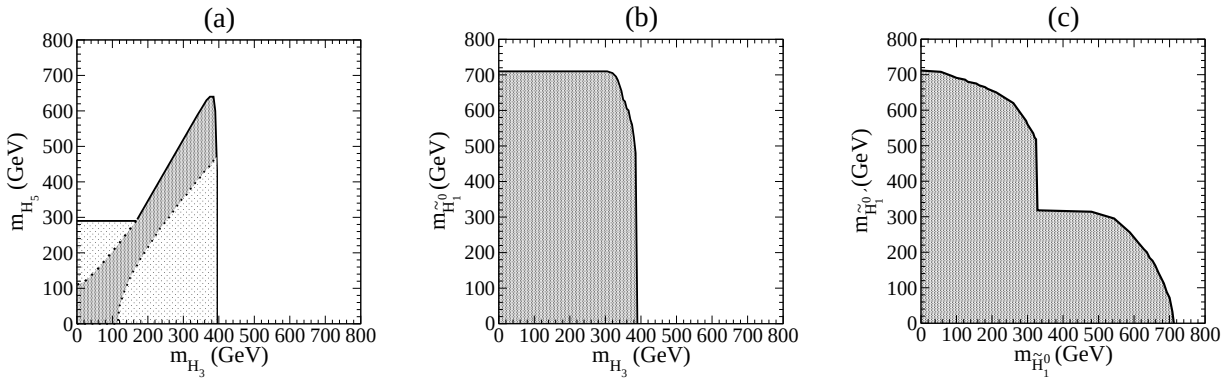

Figure 1: Allowed regions of the masses of the Higgs bosons in the m_{H_3} - m_{H_5} plane (a), in the m_{H_3} - $m_{\tilde{H}_1^0}$ plane (b) and in the $m_{\tilde{H}_1^0}$ - $m_{\tilde{H}_1^{0\prime}}$ plane (c). In Fig. 1(a) the light shadowed regions are excluded by the $Zb\bar{b}$ results.

and the mixing angles for $0 < \theta_H \leq \pi/2$ and $-\pi/2 < \alpha \leq \pi/2$. In each figure, the conditions of perturbative unitarity in Eq.(3.24) are satisfied inside the regions. In Fig. 1(a), light shadowed region is excluded by the $Z \to b\bar{b}$ result.

Fig. 1(a) shows that m_{H_3} and m_{H_5} are bounded from above respectively by about 400 GeV and about 700 GeV. These upper bound come from $|x_1^{\pm}| < 8\pi$, which give the most stringent constraint among the inequations in Eq.(4.108). For $m_{H_3} \gtrsim 170$ GeV, m_{H_5} is bounded from above whose border is approximately corresponding to $\lambda_4 \simeq 0$ or $m_{H_5} \simeq \sqrt{3} m_{H_3}$ with $\theta_H \simeq 0$. Owing to the factor $\sqrt{3}$, the more strict constraint is given on m_{H_3} than on m_{H_5}. For $m_{H_3} \lesssim 170$ GeV, on the other hand, the upper bound on m_{H_5} (290 GeV) is realized at $\theta_H \simeq \pi/2$. When all masses other than m_{H_3} are zero, m_{H_3} is bounded by $m_{H_3} < \sqrt{2\pi/3}\, v$ ($\simeq 356$ GeV) from $|x_1^{\pm}| < 8\pi$. However numerical analysis shows that the actual upper bound is a few decade GeV greater. This excess comes from some delicate cancellation in Eq.(3.96). When we impose the experimental data from $Z \to b\bar{b}$ which give the constraint on the combination of m_{H_3} and θ_H [11], the allowed region is further limited in the dark shadowed regions. The upper bounds on m_{H_3} and m_{H_5} do not change, but the remained allowed region is in the vicinity of $m_{H_5} \simeq \sqrt{3} m_{H_3}$.

In Fig. 1(b) we can see that the upper bound on $m_{\tilde{H}_1^0}$ is about 710 GeV, which is almost the same as that on the mass of the SM Higgs boson [13]. Larger values of $m_{\tilde{H}_1^0}$ are allowed for smaller values of α and θ as well as smaller m_{H_5} and $m_{\tilde{H}_1^{0\prime}}$ values. For instance, taking the limit $\alpha \to 0$, $\theta_H \to 0$, $m_{H_5} \to 0$ and $m_{\tilde{H}_1^{0\prime}} \to 0$, we obtain $m_{\tilde{H}_1^0} < \sqrt{8\pi/3}\, v$ ($\simeq 712$ GeV) in the condition $|x_1^{+}| < 8\pi$. The mass bound for another singlet $\tilde{H}_1^{0\prime}$ can be obtained by replacing $m_{\tilde{H}_1^0}$ with $m_{\tilde{H}_1^{0\prime}}$ and α with $\alpha + \pi/2$, which can be seen from Eqs.(2.19)-(2.21). Consequently the allowed regions in the m_{H_3} - $m_{\tilde{H}_1^{0\prime}}$ plane are given by the same as in Fig. 1(b). We find that contrary to the result in Fig. 1(a) there is only few difference in the case where we include the $Z \to b\bar{b}$ data.

The allowed region in the $m_{\tilde{H}_1^0}$ - $m_{\tilde{H}_1^{0\prime}}$ plane in Fig. 1(c) is symmetrical about the line of $m_{\tilde{H}_1^0} = m_{\tilde{H}_1^{0\prime}} (\equiv m)$. It is notable that at least one singlet receives very strict constraint from

perturbative unitarity. The mass of lighter singlet, either $\tilde{H}_1^0$ or $\tilde{H}_1^{0'}$, is bounded from above by 322 GeV. In analytic calculation, this upper bound is obtained as $m < \sqrt{6\pi/11}\, v$ ($\simeq 322$ GeV) from $|x_1^{\pm}| < 8\pi$.

In the following, we evaluate the upper bound on $m_{\rm lightest}$ $\left[\equiv {\rm Min}\left(m_{H_3}, m_{H_5}, m_{\tilde{H}_1^0}, m_{\tilde{H}_1^{0'}}\right)\right]$. We start from the case in which the constraints from the $Zb\bar{b}$ results are switched off. When the 3-plet is the lightest, we obtain the upper bound on $m_{\rm lightest}(= m_{H_3})$ as

$$m_{\rm lightest} < 269 \text{ GeV}, \tag{4.109}$$

which is considerably lower than that of the SM Higgs boson, 712 GeV. This condition comes from the constraints $|x_1^+| < 8\pi$ and $|x_5^-| < 8\pi$. Similar analysis has been done for $m_{\rm lightest} = m_{H_5}, m_{\tilde{H}_1^0}$ and $m_{\tilde{H}_1^{0'}}$ in order, and the same bound as in Eq.(4.109) is derived for each case. When $m_{\rm lightest} \simeq$ 269 GeV, all the masses are degenerate in mass ($m_{H_3} = m_{H_5} = m_{\tilde{H}_1^0} = m_{\tilde{H}_1^{0'}}$). The situation turns out to be quite similar to the situation of the two-Higgs-doublet model with the discrete symmetry, where the lightest of all Higgs masses are bounded at 410 GeV [16]. In the case of the GM model the number of the two-body states is greater than that in the two-Higgs-doublet model. (The neutral two body states are 14 channels in the two-Higgs-doublet model and 25 channels in the GM model.) Thereby we have obtained the stronger bounds than the two-Higgs-doublet model. Finally, when we take into account the $Zb\bar{b}$ results [11], the angle θ_H is more limited for smaller values of m_{H_3}. Consequently, the combined upper bound on $m_{\rm lightest}$ becomes lower than 269 GeV. Depending on what the lightest is, the combined upper bound turns out to be about 249 GeV (176 GeV) when m_{H_3}, $m_{\tilde{H}_1^0}$ or $m_{\tilde{H}_1^{0'}}$ (m_{H_5}) is the lightest.

We have not included the LEP direct search results, which give the lower bound $m_{H_{\rm SM}} > 114$ GeV in the SM [38]. In the GM model similar lower mass bounds can be obtained for neutral Higgs bosons but depending on the mixing angles, which would slightly affect the upper bounds by using the results in Figs. 1(a), (b) and (c). We have taken into account only the $Z \to b\bar{b}$ result as the experimental constraint [11], because this constraint drastically changes the bound in the m_{H_3}-m_{H_5} plane and also that on $m_{\rm lightest}$.

5 Conclusions

In this paper, we have analyzed unitarity constraints on the Higgs boson masses in the GM model, which includes a real and a complex isospin triplet fields but predicts $\rho = 1$ at tree level. All possible two-body elastic-scattering channels (91 channels) have been taken into account to construct the S-wave amplitude matrix in the high energy limit. The condition of S-wave unitarity in Eq.(4.108) has been applied to the eigenmatrix.

We have found that all the Higgs bosons receive their masses from the VEV under the discrete Z_2 symmetry, so that all the masses can be bounded from above by the condition of parturbative unitarity. In particular, the upper bound on the mass of the $SU(2)_{\rm V}$ 3-plet is about $1/\sqrt{3}$ lower than that on the SM Higgs boson mass (712 GeV). Hence at least one of the singly-charged Higgs boson masses is bounded from above at about 400 GeV. The mass of the lighter $SU(2)_{\rm V}$ singlet scalar state, either $\tilde{H}_0$ or $\tilde{H}_0'$, turns out to be bounded from above by about 300 GeV. Furthermore, the mass of the lightest Higgs boson among the 5-plet, the 3-plet and the two singlet states, whatever it would be, receives very strong constraint from above; i.e., $m_{\rm lightest} \simeq 270$ GeV.

The point of the parameter space at which $m_{\rm lightest}$ takes its maximum value corresponds to that where all the mass parameters are degenerate. The combined upper bound with the $Zb\bar{b}$ results becomes about 150 GeV (95% C.L.). Therefore, the model turns out to be well testable at collider experiments. The $SU(2)_{\rm V}$ 5-plet and 3-plet have the doubly- and singly-charged states, so that the distinctive phenomenological features of this model should also appear in physics of charged Higgs bosons. Detailed phenomenological features will be discussed elsewhere.

In the analysis above, we have considered the Higgs potential with the Z_2 symmetry, neglecting the trilinear scalar terms of μ_1 and μ_2. The imposition of the Z_2 symmetry in our analysis would be justified to avoid large excess of the neutrino masses. When we do not respect the Z_2 symmetry, the upper bounds in above results become relaxed according to the scales of μ_1 and μ_2 which have linear mass dimension. Unless μ_1 and μ_2 are substantially larger than $\mathcal{O}(100)$ GeV, our results above can sufficiently be applied by small relaxation.

Finally, in this paper, we have employed partial wave unitarity to constrain parameters of the GM model at the tree level. A more detailed study with the radiative effects such as vacuum stability or triviality might give more strict bounds on the Higgs boson masses in this model.

Acknowledgments

The work of M. A. was supported, in part, by Japan Society for the Promotion of Science. The work of S. K. was supported, in part, by Grant-in-Aid of the Ministry of Education, Culture, Sports, Science and Technology, Government of Japan, No. 18034004, and by Grant-in-Aid for Scientific Research, Japan Society for the Promotion of Science, No. 19540277.

References

[1] E. Gildener and S. Weinberg, Phys. Rev. D **13**, 3333 (1976).

[2] J. F. Gunion, H. E. Haber, G. L. Kane and S. Dawson, *The Higgs Hunter's Guide*, (Addison-Wesley, New York, 1990), arXiv:hep-ph/9302272.

[3] H. Georgi and M. Machacek, Nucl. Phys. B **262**, 463 (1985).

[4] M. S. Chanowitz and M. Golden, Phys. Lett. B **165**, 105 (1985).

[5] J. F. Gunion, R. Vega and J. Wudka, Phys. Rev. D **42**, 1673 (1990).

[6] R. Vega and D. A. Dicus, Nucl. Phys. B **329**, 533 (1990).

[7] J. F. Gunion, R. Vega and J. Wudka, Phys. Rev. D **43**, 2322 (1991).

[8] R. Godbole, B. Mukhopadhyaya and M. Nowakowski, Phys. Lett. B **352**, 388 (1995) [arXiv:hep-ph/9411324].

[9] K. Cheung, R. J. N. Phillips and A. Pilaftsis, Phys. Rev. D **51**, 4731 (1995) [arXiv:hep-ph/9411333].

[10] A. G. Akeroyd, Phys. Lett. B **442**, 335 (1998) [arXiv:hep-ph/9807409].

[11] H. E. Haber and H. E. Logan, Phys. Rev. D **62**, 015011 (2000) [arXiv:hep-ph/9909335].

[12] K. Cheung and D. K. Ghosh, JHEP **0211**, 048 (2002) [arXiv:hep-ph/0208254].

[13] B. W. Lee, C. Quigg and H. B. Thacker, Phys. Rev. Lett. **38**, 883 (1977); Phys. Rev. D **16**, 1519 (1977).

[14] D. A. Dicus and V. S. Mathur, Phys. Rev. D **7**, 3111 (1973).

[15] M. Lindner, Z. Phys. C **31**, 295 (1986); N. Cabibbo, L. Maiani, G. Parisi and R. Petronzio, Nucl. Phys. B **158**, 295 (1979).

[16] S. Kanemura, T. Kubota and E. Takasugi, Phys. Lett. B **313**, 155 (1993) [arXiv:hep-ph/9303263].

[17] H. Hüffel and G. Pocsik, Z. Phys. C **8** (1981) 13; J. Maalampi, J. Sirkka and I. Vilja, Phys. Lett. B **265** (1991) 371; A. Akeroyd, A. Arhrib, E.-M. Naimi, Phys. Lett. B **490** (2000) 119; I. F. Ginzburg, I. P. Ivanov, hep-ph/0312374. I. F. Ginzburg and I. P. Ivanov, Phys. Rev. D **72**, 115010 (2005) [arXiv:hep-ph/0508020];

[18] H. Komatsu, Prog. Theor. Phys. **67**, 1177 (1982); R.A. Flores and M. Sher, Ann. Phys. (NY), 148 (1983) 295; M. Sher, Phys. Rept. **179**, 273 (1989); D. Kominis and R. S. Chivukula, Phys. Lett. B **304**, 152 (1993) [arXiv:hep-ph/9301222];

[19] S. Nie and M. Sher, Phys. Lett. B **449**, 89 (1999) [arXiv:hep-ph/9811234]. S. Kanemura, T. Kasai and Y. Okada, Phys. Lett. B **471**, 182 (1999) [arXiv:hep-ph/9903289].

[20] J. R. Forshaw, A. Sabio Vera and B. E. White, JHEP **0306**, 059 (2003) [arXiv:hep-ph/0302256].

[21] S. L. Glashow and S. Weinberg, Phys. Rev. D **15**, 1958 (1977).

[22] E. J. Chun, K. Y. Lee and S. C. Park, Phys. Lett. B **566**, 142 (2003) [arXiv:hep-ph/0304069]; P. Q. Hung, Phys. Lett. B **649**, 275 (2007) [arXiv:hep-ph/0612004].

[23] M. Aoki and S. Kanemura, Work in progress.

[24] A. Kundu and B. Mukhopadhyaya, Int. J. Mod. Phys. A **11**, 5221 (1996) [arXiv:hep-ph/9507305].

[25] D. Chakraverty and A. Kundu, Mod. Phys. Lett. A **11**, 675 (1996) [arXiv:hep-ph/9508234].

[26] J. A. Grifols and A. Mendez, Phys. Rev. D **22**, 1725 (1980).

[27] B. Mukhopadhyaya, Phys. Lett. B **252**, 123 (1990).

[28] E. Asakawa and S. Kanemura, Phys. Lett. B **626**, 111 (2005) [arXiv:hep-ph/0506310]; E. Asakawa, S. Kanemura and J. Kanzaki, Phys. Rev. D **75**, 075022 (2007) [arXiv:hep-ph/0612271].

[29] M. C. Peyranere, H. E. Haber and P. Irulegui, Phys. Rev. D **44**, 191 (1991); A. Mendez and A. Pomarol, Nucl. Phys. B **349**, 369 (1991); S. Kanemura, Phys. Rev. D **61**, 095001 (2000) [arXiv:hep-ph/9710237]; A. Arhrib, R. Benbrik and M. Chabab, J. Phys. G **34**, 907 (2007) [arXiv:hep-ph/0607182]; A. Arhrib, R. Benbrik and M. Chabab, Phys. Lett. B **644**, 248 (2007) [arXiv:hep-ph/0701126].

[30] S. Kanemura, Eur. Phys. J. C **17**, 473 (2000) [arXiv:hep-ph/9911541]; A. Arhrib, M. Capdequi Peyranere, W. Hollik and G. Moultaka, Nucl. Phys. B **581**, 34 (2000) [Erratum-ibid. **2004**, 400 (2004)] [arXiv:hep-ph/9912527]; H. E. Logan and S. Su, Phys. Rev. D **66**, 035001 (2002) [arXiv:hep-ph/0203270]; O. Brein, arXiv:hep-ph/0209124; O. Brein and T. Hahn, Eur. Phys. J. **52**, 397 (2007) [arXiv:hep-ph/0610079].

[31] S. Kanemura, S. Moretti and K. Odagiri, JHEP **0102**, 011 (2001) [arXiv:hep-ph/0012030].

[32] J. F. Gunion, J. Grifols, A. Mendez, B. Kayser and F. I. Olness, Phys. Rev. D **40**, 1546 (1989); J. F. Gunion, C. Loomis and K. T. Pitts, arXiv:hep-ph/9610237; G. Azuelos, K. Benslama and J. Ferland, J. Phys. G **32**, 73 (2006) [arXiv:hep-ph/0503096]; A. Hektor, M. Kadastik, M. Muntel, M. Raidal and L. Rebane, Nucl. Phys. B **787**, 198 (2007) [arXiv:0705.1495 [hep-ph]]; T. Han, B. Mukhopadhyaya, Z. Si and K. Wang, Phys. Rev. D **76**, 075013 (2007) [arXiv:0706.0441 [hep-ph]].

[33] B. Dion, T. Gregoire, D. London, L. Marleau and H. Nadeau, Phys. Rev. D **59**, 075006 (1999) [arXiv:hep-ph/9810534].

[34] A. G. Akeroyd and M. Aoki, Phys. Rev. D **72**, 035011 (2005) [arXiv:hep-ph/0506176].

[35] K. Huitu, J. Laitinen, J. Maalampi and N. Romanenko, Nucl. Phys. B **598**, 13 (2001) [arXiv:hep-ph/0006261]; J. Maalampi and N. Romanenko, Phys. Lett. B **532**, 202 (2002) [arXiv:hep-ph/0201196].

[36] J. F. Gunion, Int. J. Mod. Phys. A **13**, 2277 (1998) [arXiv:hep-ph/9803222]; S. Chakrabarti, D. Choudhury, R. M. Godbole and B. Mukhopadhyaya, Phys. Lett. B **434**, 347 (1998) [arXiv:hep-ph/9804297]; J. E. Cieza Montalvo, N. V. . Cortez, J. Sa Borges and M. D. Tonasse, Nucl. Phys. A **790**, 554 (2007) [arXiv:hep-ph/0612039]; C. X. Yue, S. Zhao and W. Ma, Nucl. Phys. B **784**, 36 (2007) [arXiv:0706.0232 [hep-ph]].

[37] J. M. Cornwall, D. N. Levin and G. Tiktopoulos, Phys. Rev. D **10**, 1145 (1974) [Erratum-ibid. D **11**, 972 (1975)].

[38] W. M. Yao *et al.* [Particle Data Group], J. Phys. G **33**, 1 (2006).